CRYSTAL GROWTH & DESIGN

Article

pubs.acs.org/crystal

Gas-Phase Modeling of Chlorine-Based Chemical Vapor Deposition of Silicon Carbide

Stefano Leone,*[,†] Olof Kordina,[†] Anne Henry,[†] Shin-ichi Nishizawa,[†,‡] Örjan Danielsson,[†,§] and Erik Janzén[†]

[†]Department of Physics, Chemistry and Biology, Linköping University, SE-58 183 Linköping, Sweden

[‡]National Institute of Advanced Industrial Science and Technology, 305-8568 Tsukuba, Japan

[§]Sandvik Heating Technology AB, Box 502, SE-734 27 Hallstahammar, Sweden

ABSTRACT: Kinetic calculations of the chemical phenomena occurring in the epitaxial growth of silicon carbide are performed in this study. The main process parameters analyzed are precursor types, growth temperature, Cl/Si ratio, and precursors' concentration. The analysis of the gas-phase reactions resulted in a model which could explain most of the already reported experimental results, performed in horizontal hot-wall reactors. The effect of using different carbon or silicon precursors is discussed, by comparing the gas-phase composition and the resulting C/Si ratio inside the hot reaction chamber. Chlorinated molecules with three chlorine atoms seem to be the most efficient and resulting in a uniform C/Si ratio along the susceptor coordinate. Further complexity in the process derives from the use of low temperatures, which affects not only the gas-phase composition but also the risk of gas-phase nucleation. The Cl/Si ratio is demonstrated to be crucial not only for the prevention of silicon clusters but also for the uniformity of the gas-phase composition.

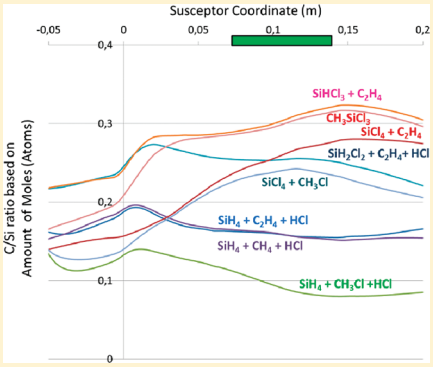

1. INTRODUCTION

The role of power electronics is constantly increasing, and it is forecasted to become predominant in the next few decades. Silicon carbide (SiC) can be one of the major actors in high power flow control and high voltage conversion, thanks to its unique physical and chemical properties. The quality and the substrate diameter of this wide band gap material keep increasing. Thick and low doped epitaxial layers are the basic requirements for high voltage devices. High cost and moderate quality of such layers still partially limit the full employment of this material. High growth rate processes are required to reduce the manufacturing cost where two main approaches are predominately used nowadays: very low pressures[1] or chlorine-based chemical vapor deposition (CVD).[2,42]

The chlorine-based CVD process is a well-established technique introduced in 2004[3,4] to grow high quality epitaxial layers of 4H-SiC at high growth rates. The effect of the main growth parameters on the epitaxial process and their tuning depending on the substrate off-angles have been broadly studied.[5,6] Different precursors can be used resulting in different process conditions, efficiency, problems, and advantages.[7] Yet this process has been developed by different groups with different reactors and process conditions.[2,4,8−11,41] At Linköping University most of the development has been carried out by testing different precursors and dopant incorporations.[2,12,13] The availability of a large number of experimental results can be very useful to support theoretical calculations such as simulation of the gas phase chemistry.

Calculations of the fluid dynamic and chemical phenomena occurring in CVD processes are very powerful tools commonly used to understand and predict the overall growth process. Modeling can support hardware improvements, such as modifications of the reaction chamber in order to reduce parasitic deposition, increase growth rate by selecting the proper precursors and growth conditions, and understand dopant incorporation or etching phenomena. Validated models can be employed to forecast results when doing major changes on the hardware for new applications, for example, bulk growth or reduced temperature processes.

Several models have been proposed for the case of SiC epitaxial growth,[14−22] but only a few have been done on the chlorine-based CVD process.[23,24] Veneroni et al. have set up the most complete study so far with predictions on the growth rate fitting well with experimental results.[25−27] Yet their study was limited to two sets or precursors (SiH_4 + C_2H_4 + HCl or $SiHCl_3$ + C_2H_4) and fixed growth conditions (such as temperature and Cl/Si ratio). Wang et al. did some calculations of the gas- and solid-phase states for the $SiCl_4$ chemistry.[28−31] Nishizawa did gas-phase calculations to compare the standard chemistry (SiH_4 + C_3H_8) with and without addition of HCl, or using $SiHCl_3$ as a silicon precursor.[32] Pons et al. studied the case of MTS (CH_3SiCl_3) in a vertical reactor for the deposition of polycrystalline SiC.[33] Nigam et al. performed only

Received: December 21, 2011
Revised: February 7, 2012
Published: February 27, 2012

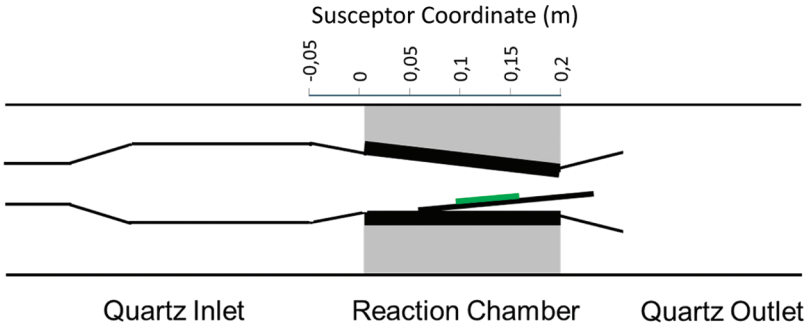

Figure 1. 2D simplified geometry of the horizontal hot-wall reactor adopted for epitaxial growth of SiC and used as boundary conditions for all the simulations. A susceptor plate is standing in the middle of the reaction chamber holding a SiC substrate (green line). Susceptor coordinates are indicated on top of the figure. The same coordinates are used for the following plots.

thermodynamic calculations for the bulk growth of SiC using $SiCl_4$.[34,35]

A thorough study of the main possible chlorinated precursors and the effect of the main process parameters for the chlorine-based CVD process is still lacking. Many unanswered questions about the growth efficiency and about process tuning of such processes still exist, such as how to explain the different efficiencies of the chlorinated and nonchlorinated precursors, their effect on growth rate, morphology, dopants incorporation; how to select the proper precursor depending on the target and process conditions; which process conditions lead to higher precursors uniformity along the reaction chamber; what are the most suitable carbon precursors for such chloride-based process. In fact, further developments are required for large area reaction chambers or bulk growth processes; therefore, such a theoretical understanding can pave the way for a faster development.

In this study, the epitaxial growth process of SiC in a horizontal hot-wall reactor is simulated with commercial software,[36] which allows detailed fluid dynamic, thermodynamic, and kinetic calculations. The gas-phase chemistry of the process is studied in detail for a different set of precursors at different growth conditions, using as boundary conditions the typical settings of the hot-wall CVD reactor employed at Linköping University.

2. REACTOR MODELING

The software used for all the calculations has been CFD-ACE +.[36] A two-dimensional (2D) geometry of the section of the same horizontal hot-wall CVD reactor used for all the growth experiments has been used as geometrical boundary conditions for the simulations (Figure 1). Both the quartz inlet and outlet were included in the calculations, although a simplified geometry has been adopted for all the parts of the reaction chamber beyond the area where the SiC substrates are usually located. An accurate grid was implemented, especially refined in correspondence with the susceptor parts where the SiC substrate is positioned.

2.1. Fluid Dynamic Settings. Flow, heat, and chemical reactions were included in the model, and no radiation or turbulence was considered. The model was solved only for gas-phase media. The volume conditions were set as follows (according to terminology used in the CFD-ACE + software):

- density = ideal gas law
- viscosity = mix kinetic theory
- specific heat = mix JANNAF method
- thermal conductivity = mix kinetic theory
- mass diffusivity = multicomponent diffusion (thermo-diffusion and conservation of species considered as well)
- reference species = hydrogen

The main boundary conditions at the inlet were

- gas speed = 0.46 m/s
- reference pressure = 200 mbar
- inlet temperature = 300 K

The heat profile in the susceptor was set according to silicon melting tests performed in the same reactor used for all the growth experiments, at the same conditions of gas flow (50 L/min) and pressure (200 mbar) used for the simulations.

All the simulations were solved until all the main species converged to a convergence criteria 4 orders of magnitudes lower than the initial value. Typically 50 000 iterations were required to solve a 2D problem.

2.2. Gas-Phase Reactions Settings. Fixed growth parameters input as boundary conditions were temperature profile, growth temperature of 1600 °C, total gas flow of 50 L/min (hydrogen as main species), process pressure of 200 mbar, C/Si ratio of 1, Cl/Si ratio of 3 (except for the case of $SiCl_4$, where the Cl/Si ratio was fixed to 4); no dopants were included in the calculations. The set of precursors used for the calculations were

- $SiH_4 + C_2H_4 + HCl$
- $SiH_4 + CH_3Cl + HCl$
- $SiH_4 + CH_4 + HCl$
- $SiH_2Cl_2 + C_2H_4 + HCl$
- $SiHCl_3 + C_2H_4$
- $SiCl_4 + C_2H_4$
- $SiCl_4 + CH_3Cl$
- CH_3SiCl_3

Further possible precursors, such as SiH_3Cl, were not considered since they are not commonly used in industry due to high production costs or process related problems.

Further calculations were done with the $SiH_4 + C_2H_4 + HCl$ chemistry: two more growth temperatures (1300 and 1900 °C) and two more Cl/Si ratios (0.5 and 10).

The database of gas-phase reactions adopted in this model was divided in three groups: silane pyrolysis; hydrocarbon pyrolysis; and chlorinated molecules decomposition. The amount of reactions employed for the calculations changed accordingly to the precursor set at the inlet mixture, as reported in Table 1. The first 88 reactions listed in the table were common for all the cases, while for some precursor sets a few more reaction steps have been added to the 88 common reactions, as described below. No organosilicon species

dx.doi.org/10.1021/cg201684e | Cryst. Growth Des. 2012, 12, 1977−1984

Table 1. List of Gas-Phase Chemical Reactions Included in the Simulations Database[a]

	reaction	A	n	E_a/R	ref
1	$CH_4 = CH_3 + H$	8.3×10^{13}	0	52246	15
	reverse rate	1.204×10^{15}	−0.4	0	15
2	$C_2H_2 = C_2H + H$	1.8×10^{15}	0	62445	15
	reverse rate	1.807×10^{14}	0	0	15
3	$C_2H_4 = C_2H_2 + H_2$	1.4×10^{12}	0.44	44670	15
	reverse rate	3.011×10^{11}	0	19600	15
4	$C_2H_5 = C_2H_4 + H$	6.31×10^{10}	0.4	19726	27
	reverse rate	8.431×10^{8}	1.49	499	15
5	$C_2H_6 = 2CH_3$	1.2×10^{22}	−1.79	45834	15
	reverse rate	1.024×10^{15}	−0.64	0	15
6	$C_3H_8 = C_2H_5 + CH_3$	2.3×10^{22}	−1.8	44637	15
	reverse rate	4.456×10^{13}	0	0	15
7	$C_2H_6 + CH_2 = C_2H_5 + CH_3$	1.2×10^{14}	0	0	15
8	$2\ CH = C_2H_2$	1.204×10^{14}	0	0	15
9	$CH_2 + H = CH + H_2$	3.011×10^{13}	0	0	15
10	$CH_2 + H_2 = CH_3 + H$	1.987×10^{13}	0.5	0	15
	reverse rate	1.987×10^{13}	0	0	15
11	$CH_2 + CH = C_2H_2 + H$	3.975×10^{13}	0	0	15
12	$2CH_2 = C_2H_4$	1.024×10^{12}	0	0	15
13	$2CH_2 = C_2H_2 + 2H$	1.084×10^{14}	0	400	15
14	$2CH_2 = C_2H_2 + H_2$	1.204×10^{13}	0	400	15
15	$CH_3 + H_2 = CH_4 + H$	289.1	3.12	4384	15
	reverse rate	13250	3	4045	15
16	$CH_3 + CH = C_2H_3 + H$	3.011×10^{13}	0	0	15
17	$CH_3 + CH_2 = C_2H_4 + H$	1.807×10^{13}	0	0	15
18	$2CH_3 = C_2H_5 + H$	1.148×10^{21}	0	13275	15
	reverse rate	3.674×10^{13}	0	0	15
19	$CH_4 + CH = C_2H_5$	1.626×10^{14}	0	0	15
20	$CH_4 + CH = C_2H_4 + H$	3.011×10^{13}	0	−200	15
21	$CH_4 + CH_2 = C_2H_6$	1.024×10^{13}	0	0	15
22	$CH_4 + CH_2 = 2CH_3$	1.265×10^{13}	0.5	0	15
23	$CH_4 + CH_3 = C_2H_5 + H_2$	1.024×10^{13}	0	11500	15
24	$C_2H + H_2 = C_2H_2 + H$	1.144×10^{13}	0	1450	15
	reverse rate	6.022×10^{13}	0	11200	15
25	$C_2H + CH_2 = C_2H_2 + CH$	1.807×10^{13}	0	0	15
26	$C_2H + CH_4 = C_2H_2 + CH_3$	1.807×10^{12}	0	250	15
	reverse rate	1.807×10^{11}	0	8700	15
27	$C_2H_2 + H = C_2H_3$	5.54×10^{12}	0	1214	15
28	$C_2H_2 + H_2 = C_2H_3 + H$	2.409×10^{12}	0	32700	15
29	$2C_2H_2 = C_2H_3 + C_2H$	9.635×10^{12}	0	42500	15
	reverse rate	9.635×10^{11}	0	0	15
30	$C_2H_3 + M = C_2H_2 + H + M$	3.011×10^{15}	0	16000	15
31	$C_2H_3 + H_2 = C_2H_4 + H$	30110	2.63	4298	15
	reverse rate	1325000	2.53	6160	15
32	$C_2H_3 + CH_2 = C_2H_2 + CH_3$	1.807×10^{13}	0	0	15
33	$C_2H_3 + CH_3 = C_2H_2 + CH_4$	3.914×10^{11}	0	0	15
34	$C_2H_3 + CH_4 = C_2H_4 + CH_3$	1.445	4.02	2754	15
	reverse rate	6.624	3.7	4780	15
35	$C_2H_4 + M = C_2H_2 + H_2 + M$	1.5×10^{15}	0	28100	15
36	$C_2H_4 + M = C_2H_3 + H + M$	1.4×10^{16}	0	41470	15
37	$C_2H_4 + H_2 = C_2H_5 + H$	1.024×10^{13}	0	34300	15
	reverse rate	1.807×10^{12}	0	0	15
38	$C_2H_4 + C_2H_2 = 2C_2H_3$	2.409×10^{13}	0	34400	15
39	$2C_2H_4 = C_2H_3 + C_2H_5$	4.818×10^{14}	0	36000	15
	reverse rate	4.818×10^{11}	0	0	15
40	$C_2H_5 + H = C_2H_6$	3.613×10^{13}	0	0	15
41	$C_2H_5 + H_2 = C_2H_6 + H$	3.071	3.6	4253	15
	reverse rate	1.445×10^{9}	1.5	3730	15
42	$C_2H_5 + CH_3 = C_2H_4 + CH_4$	1.987×10^{13}	0.5	0	15
43	$C_2H_5 + CH_4 = C_2H_6 + CH_3$	0.08618	4.14	6322	15
	reverse rate	1.506×10^{-7}	6	3730	15
44	$C_2H_5 + C_2H = C_2H_2 + C_2H_4$	1.807×10^{12}	0	0	15
45	$C_2H_5 + C_2H_2 = C_2H + C_2H_6$	2.71×10^{11}	0	11800	15
	reverse rate	3.613×10^{12}	0	0	15
46	$C_2H_5 + C_2H_3 = C_2H_2 + C_2H_6$	4.818×10^{11}	0	0	15
47	$C_2H_5 + C_2H_4 = C_2H_6 + C_2H_3$	662.4	3.13	9063	15
	reverse rate	602.2	3.3	5285	15
48	$2C_2H_5 = C_2H_6 + C_2H_4$	7.227×10^{12}	0	540	15
	reverse rate				15
49	$Si_2H_6 = Si_2H_4 + H_2$	9.09×10^{9}	1.8	27290	15
	reverse rate	6.624×10^{13}	0	0	15
50	$SiH_4 = SiH_2 + H_2$	3.12×10^{9}	1.7	27550	15
51	$Si_2 = 2Si$	1×10^{15}	0	37460	15
52	$Si_2H_4 = Si + SiH_4$	1.42×10^{13}	0.54	28980	15
53	$Si_2H_4 = Si_2H_2 + H_2$	3.16×10^{14}	0	26690	15
	reverse rate	2.45×10^{14}	0	1000	15
54	$Si_2H_6 = SiH_2 + SiH_4$	1.81×10^{10}	1.7	25280	15
55	$Si_3H_8 = SiH_2 + Si_2H_6$	6.97×10^{12}	1	26525	15
56	$SiH_2 + H = SiH + H_2$	1.204×10^{13}	0	0	15
57	$SiH_2 + Si = Si_2 + H_2$	1.5×10^{14}	0	0	15
58	$SiH_2 + Si = Si_2H_2$	7.24×10^{12}	0	1000	15
59	$2SiH_2 = Si_2H_2 + H_2$	6.5×10^{14}	0	0	15
60	$SiH_4 + Si = 2SiH_2$	9.31×10^{12}	0	1000	15
61	$SiH_4 + Si = Si_2H_2 + H_2$	1.5×10^{14}	0	3670	15
62	$SiH_4 + SiH = Si_2H_4 + H$	3×10^{14}	0	4535	15
63	$SiH_4 + SiH = Si_2H_5$	4.139×10^{14}	0	0	15
64	$Si_2 + H = Si + SiH$	5.15×10^{13}	0	2670	15
65	$Si_2 + H_2 = 2SiH$	1.54×10^{13}	0	20140	15
66	$Si_2 + H_2 = Si_2H_2$	1.54×10^{13}	0	1000	15
67	$Si_2H_4 + H_2 = SiH_2 + SiH_4$	9.41×10^{13}	0	0	15
	reverse rate	9.43×10^{10}	1.1	2916	15
68	$Si_2H_4 + SiH_4 = SiH_2 + Si_2H_6$	1.73×10^{14}	0.4	0	15
	reverse rate	2.65×10^{15}	0.1	4267	15
69	$Si_2H_6 + H \rightarrow Si_2H_5 + H_2$	1.445×10^{14}	0	1250	15
70	$Si_2H_6 + Si = SiH_2 + Si_2H_4$	1.3×10^{15}	0	6345	15
71	$H_2 + H = 3H$	2.228×10^{14}	0	48350	15
	reverse rate	9.792×10^{17}	−1	0	15
72	$2H_2 = 2H + H_2$	9.033×10^{14}	0	48350	15
	reverse rate	9.792×10^{16}	−0.6	0	15
73	$2H + M = H_2 + M$	5.44×10^{18}	−1.3	0	15
74	$SiH_3Cl = HCl + SiH_2$	4.898×10^{14}	0	37993	25
75	$SiH_3Cl = H_2 + SiHCl$	3.89×10^{14}	0	32709	15
	reverse rate	2.63×10^{14}	0	9108	15
76	$SiH_2Cl_2 = SiCl_2 + H_2$	8.318×10^{13}	0	38942	15
77	$SiH_2Cl_2 = SiHCl + HCl$	6.918×10^{14}	0	38137	15
78	$SiHCl + H \rightarrow SiH + HCl$	8.511×10^{13}	0	8036	15
79	$SiCl + HCl \rightarrow SiCl_2 + H$	1.995×10^{13}	0	9808	15
80	$SiCl + H_2 \rightarrow SiHCl + H$	3.981×10^{14}	0	16400	25
81	$HCl = H + Cl$	4.365×10^{13}	0	41129	25
82	$Cl + H_2 = HCl + H$	4.786×10^{13}	0	2646	25
83	$Si + HCl = SiCl + H$	9.55×10^{14}	0	6949	25
84	$Si + H_2 = SiH_2$	1.202×10^{12}	0.5	0	27
85	$SiH_2 + HCl = SiCl + 3H$	1.862×10^{13}	0	8097	25
86	$SiHCl_3 = SiCl_2 + HCl$	4.898×10^{14}	0	37079	25
87	$SiHCl_3 + H = SiCl_3 + H_2$	2.455×10^{12}	0	1274	25
88	$SiCl_4 = Cl + SiCl_3$	4.786×10^{15}	0	55937	25
89	$CH_3SiCl_3 = CH_3 + SiCl_3$	1.72×10^{14}	0	41163	33
90	$CH_3SiCl_3 + Cl = CH_2SiCl_3 + HCl$	8250000	2	755	33
91	$CH_3SiCl_2 + HCl = CH_3SiCl_3 + H$	5×10^{11}	0	9058	33

dx.doi.org/10.1021/cg201684e | Cryst. Growth Des. 2012, 12, 1977−1984

Table 1. continued

	reaction	A	n	E_a/R	ref
92	$CH_3SiCl_3 + CH_3 = CH_2SiCl_3 + CH_4$	0.25	4	4177	33
93	$CH_3SiCl_3 + SiCl_3 = SiCl_4 + CH_3SiCl_2$	1.6×10^9	0	1812	33
94	$CH_3SiCl_2 + SiCl_3 = SiCl_2 + CH_3SiCl_3$	3×10^{13}	0	22745	33
95	$CH_3SiCl_2 + SiCl_3 = SiCl_4 + CH_3SiCl$	1.3×10^{14}	0	25161	33
96	$CH_3SiHCl_2 = CH_3SiCl + HCl$	1×10^{16}	0	39855	33
97	$CH_2SiCl_3 + H_2 = CH_3SiCl_3 + H$	290	3.1	4378	33
98	$2CH_3Cl + H_2 = 2CH_3 + 2HCl$	1.26×10^{15}	0	37741	40
99	$CH_3Cl = CH_3 + Cl$	1.4×10^{15}	0	41346	40

[a]The rate constants are written according to Arrhenius equation: $K = AT^n e^{-E_a/RT}$. The system of units used is CGS. All reactions are governed by equilibrium unless indicated by an arrow. Third body reactants are indicated by M. Whereas reverse rates are not indicated, they are calculated from equilibrium thermochemistry. The main parameters adopted for the calculations are listed in paragraph 2.

reactions were included in the calculations, since preliminary calculations indicated a negligible formation of such species. A fixed set of reactions has been used for all cases:

- 48 carbon gas-phase reactions
- 23 silicon gas-phase reactions
- 3 hydrogen gas-phase reactions
- 12 chlorine-related gas-phase reactions
- In case of MTS: 9 more reactions were added (reactions 89–97)
- In case of CH_3Cl: 2 more reactions were added (reactions 98 and 99)

The chemical species considered were

- 11 carbon species
- 10 silicon species
- 2 hydrogen species
- 12 chlorinated species
- In case of CH_3Cl: 1 more species was included
- In case of MTS: 4 more species were included

In this study no surface reaction mechanism has been included. Yet the results achieved and trends obtained by studying only the gas-phase are in good agreement with our experimental results on the epitaxial process. A lot of information could be found by comparing the results from the different calculations described in the next section. Further optimization of the model and of the surface reaction mechanism will be discussed in a future work.

3. RESULTS AND DISCUSSION

As mentioned in the previous section, most of the growth conditions (i.e., boundary conditions of the simulations) were kept fixed for each calculation. For each case, the total amount of each gas species formed inside the reaction chamber could be calculated. In order to obtain a detailed view of which species get very close to the SiC substrate during the growth process, we have analyzed the amount of each species formed at the bottom of the susceptor including the place where the SiC substrate is located (as indicated in Figure 1), along the susceptor coordinates. These are the species that can diffuse through the stagnant layer formed in the gas phase; they can be absorbed on the wafer and either undergo further decomposition through surface reactions or are immediately desorbed. It has to be taken into account that, due to the effect of thermal diffusion, smaller molecules will be more abundant in the hotter part, that is at the susceptor walls, and vice versa.

This discussion will be divided in four parts. The first two will focus on the resulting gas-phase chemistry when using different sets of precursors. Five different silicon precursors will be compared first and then three carbon precursors. In all cases the following growth parameters are kept fixed (T = 1600 °C, C/Si ratio = 1, Cl/Si ratio = 3, H_2 = 50 L/min, P = 200 mbar). In the other two parts, the effect on the growth process of two main growth parameters, that is, the process temperature and the Cl/Si ratio, will be compared and discussed. In these two last cases, the set of precursors used is the one with SiH_4 + C_2H_4 + HCl.

3.1. Silicon Precursors. Five different silicon precursors were considered: SiH_4, SiH_2Cl_2, $SiHCl_3$, $SiCl_4$, and CH_3SiCl_3.

Three cases of this comparison are shown in Figure 2. In all cases, $SiCl_2$ is the most abundant silicon intermediate, while C_2H_2 is the only carbon intermediate with a concentration that is unaffected by the silicon precursor. The simplest case, that is, addition of HCl to the standard precursors (Figure 2a), shows the most complex gas phase composition; monatomic silicon is here more abundant than in all the other cases, which means that the formation of clusters in the gas phase may occur. Our growth experiments indeed confirm this, since Cl/Si ratios higher than 3 are often required in order to avoid silicon cluster formation.[42] The amount of monatomic silicon decreases by increasing the number of chlorine atoms in the silicon precursor with $SiCl_4$ being the one with the lowest amount of monatomic silicon formed, with a molar fraction below 10^{-4} (Figure 2b). MTS (CH_3SiCl_3) (Figure 2c) and $SiHCl_3$ give very similar profiles, which is expected since MTS cracks very efficiently into $SiCl_3$ and subsequently into $SiCl_2$, exactly as $SiHCl_3$ does. Similar results were found in another study.[43] SiH_2Cl_2 has an intermediate gas-phase chemistry compared to the HCl-addition case and $SiHCl_3$. SiH_2Cl_2 has a significant chance for silicon cluster formation. $SiCl_4$ is a well-known stable molecule in this temperature regime, and this causes its cracking in the reaction chamber to occur a bit later than in the other cases. This eventually results in a nonuniform concentration of $SiCl_2$ along the susceptor. Overall the gas-phase chemistry becomes simpler with the molecules having more chlorine atoms; yet from a uniformity point of view, TCS and MTS are probably the ones giving the steadiest and most uniform gas-phase composition as will be shown later.

3.2. Carbon Precursors. Three different carbon precursors were considered: C_2H_4, CH_3Cl, and CH_4.

The results obtained by these precursors, in combination with SiH_4 and HCl, are quite similar. In all cases C_2H_2 is the only relevant carbon intermediate (molar fraction above 10^{-4}) in the central and hotter part of the susceptor. When using CH_3Cl, a not very steady profile of C_2H_2 is observed along the susceptor coordinates. Even if CH_3Cl cracks almost immediately into the radical CH_3, C_2H_2 is the most thermodynamic stable species in this temperature regime; therefore its formation is straightforward. This result is in agreement with

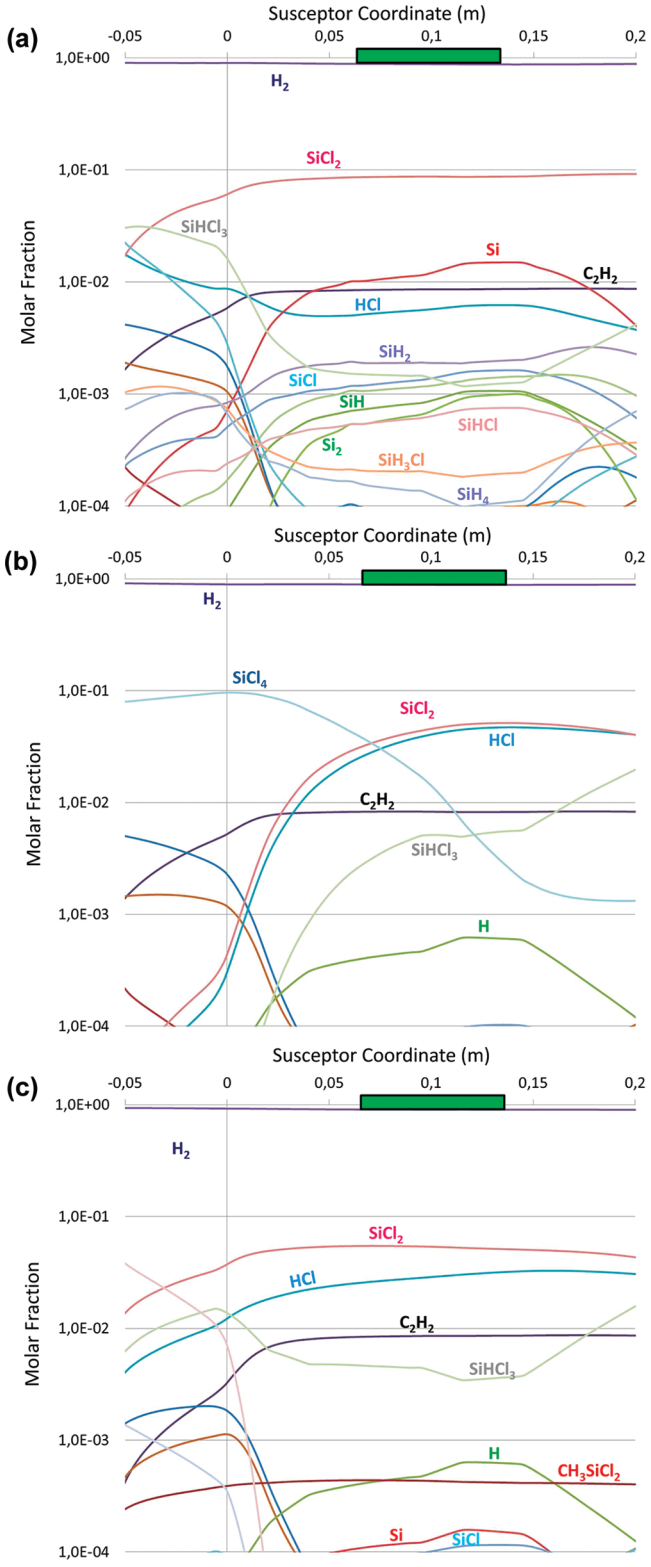

Figure 2. Plot of the gas-phase composition along the susceptor coordinates for different silicon precursors: (a) $SiH_4 + C_2H_4 + HCl$; (b) $SiCl_4 + C_2H_4$; (c) CH_3SiCl_3. The SiC substrate is indicated by the rectangular box positioned between 0.08 and 0.13 m on the top coordinate. In all the cases the Si/H_2 ratio was fixed at 0.15%, and C/Si ratio at 1. The Cl/Si ratio is also fixed at 3, except for case (b) when considering $SiCl_4$ as a precursor.

previous studies based on thermodynamic calculations, which indicated that species such as CH_4,[19] but also SiC_2 and Si_2C,[38] could be omitted from kinetic calculations. Yet these results do partially contradict our experimental results. Simulations on a 3D model, integrated with surface reactions, may be needed.

In Figure 3 the resulting C/Si ratio for the different sets of precursors analyzed is displayed. The C/Si ratio was calculated

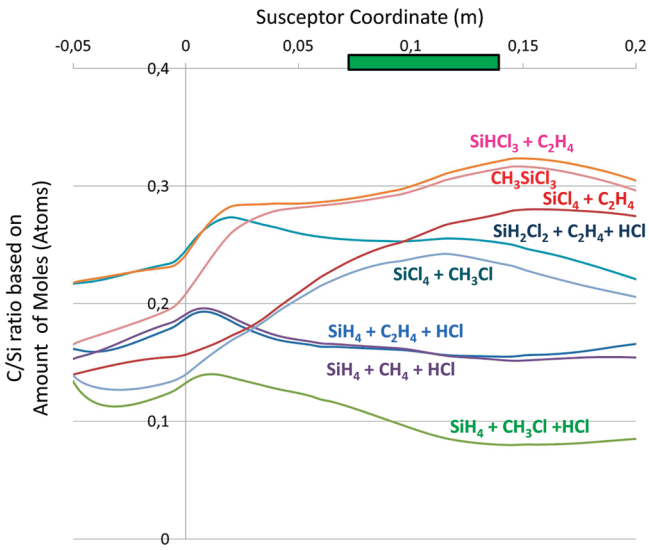

Figure 3. Plot of the gas-phase C/Si ratio along the susceptor coordinates for different precursors.

as the ratio between the total amount of carbon and silicon moles formed in the gas phase. It is important to observe once more that the amount of species used for this comparison is that existing at the susceptor bottom wall, where the SiC substrate is located. As may be seen in the plot, its values are well below the stoichiometric unity introduced as gas mixture at the inlet, which is probably because thermal diffusion redistributes the species inside the reaction chamber according to several parameters, such as their mass and heat capacity. In this figure, it is relevant to notice that MTS and $SiHCl_3$ ensure a more stoichiometric precursor supply compared to the other precursors, $SiCl_4$ gives the least uniform C/Si ratio, while the HCl-added precursors are the most uniform. In all cases, hydrocarbons (C_2H_4 and CH_4) work slightly better than CH_3Cl does.

3.3. Temperature Effect. Comparing the gas-phase compositions obtained at different temperatures (1300 °C; 1600 °C; 1900 °C), it appears clear that growing at 1600 °C leads to a less complex chemistry. Although in all cases $SiCl_2$ and C_2H_2 are still the most relevant intermediates, their profiles along the susceptor are no longer steady when growing at 1300 or 1900 °C. At low temperature (1300 °C), the carbon chemistry becomes much more complicated: non-decomposed precursors and radicals such as CH_3 are almost comparable in concentration to C_2H_2, which hence creates a nonuniform profile. $SiCl_2$ is still by far the most abundant species, but more intermediate chlorosilanes exist in relatively large amounts. Our growth experiments at 1300 °C[37] demonstrate how critical the surface mobility and carbon absorption are at this temperature, making any conclusion on the effect of gas-phase chemistry difficult.

At high temperature (1900 °C) maybe more reactions should be taken into account, especially those considering the formation of Si_2C and SiC_2. In our simplified calculation, it comes out

dx.doi.org/10.1021/cg201684e | Cryst. Growth Des. 2012, 12, 1977−1984

clear that all the monatomic and biatomic species become more important, yet $SiCl_2$ and C_2H_2 are still the main actors.

It is interesting to discuss the effect of the temperature on the C/Si ratio if only the most important species contributing to the growth are considered. According to Fiorucci et al.,[27] $SiCl_2$ − SiCl − Si are the most important silicon species, while C_2H_2 − CH_4 − CH are the most relevant carbon species. A plot of the "effective" C/Si ratio, calculated only with the above species, is shown in Figure 4. The low temperature

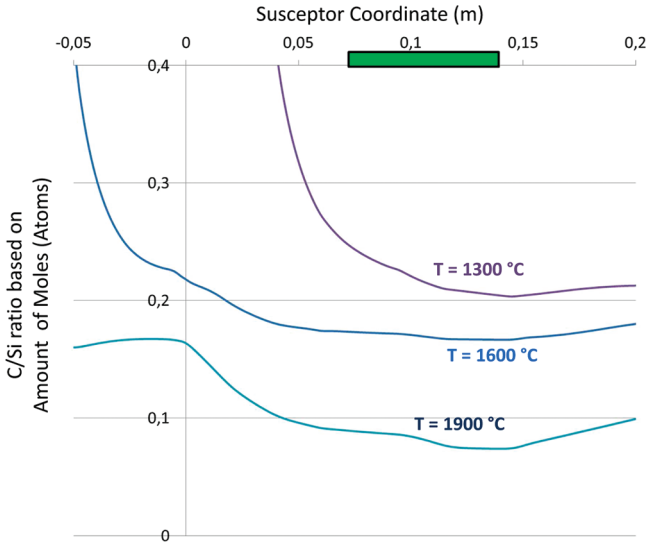

Figure 4. Plot of the effective C/Si ratio at three different temperatures: 1300 °C; 1600 °C; 1900 °C. This ratio is calculated by the amount of the most important intermediates: $SiCl_2$ − SiCl − Si, and C_2H_2 − CH_4 − CH. The precursors are SiH_4 + C_2H_4 + HCl.

process appears to be more difficult to control in terms of uniformity, being very carbon rich especially in the upstream part of the reaction chamber. At 1600 and 1900 °C, the cracking of the precursors has occurred efficiently and no relevant difference can be found.

3.4. Cl/Si Ratio. As expected the main effect of increasing the Cl/Si ratio from 0.5 to 3 and even 10 is to reduce the presence of monatomic silicon and increase the concentration of $SiCl_2$, as seen in Figure 5. Obviously the carbon chemistry is not affected. At the lowest ratio of 0.5 (Figure 5a), which can be considered almost as no chlorine presence in the system, the concentration of monatomic silicon is comparable with that of $SiCl_2$, and this makes the chance of silicon droplets formation in the gas phase very likely. The amount of HCl is higher for a Cl/Si ratio of 10 (Figure 5b), yet most of the HCl is consumed in the formation of chlorinated silicon species. Etching effects are definitively going to become more important at these conditions, but not as dramatic as expected.

In Figure 6 the C/Si ratio is plotted for the three different Cl/Si ratios analyzed by calculations. As mentioned above, the growth with Cl/Si = 0.5 could be regarded almost as the standard process, that is, with no addition of chlorine, and it can be clearly seen that the C/Si ratio uniformity along the susceptor is the worst. The comparison shows that higher amounts of chlorine result in a better uniformity of the C/Si ratio. The explanation may be found in the more uniform concentration of $SiCl_2$ which, on account of the presence of chlorine, gradually becomes the only significant silicon intermediate as the concentration of chlorine is increased. This result demonstrates

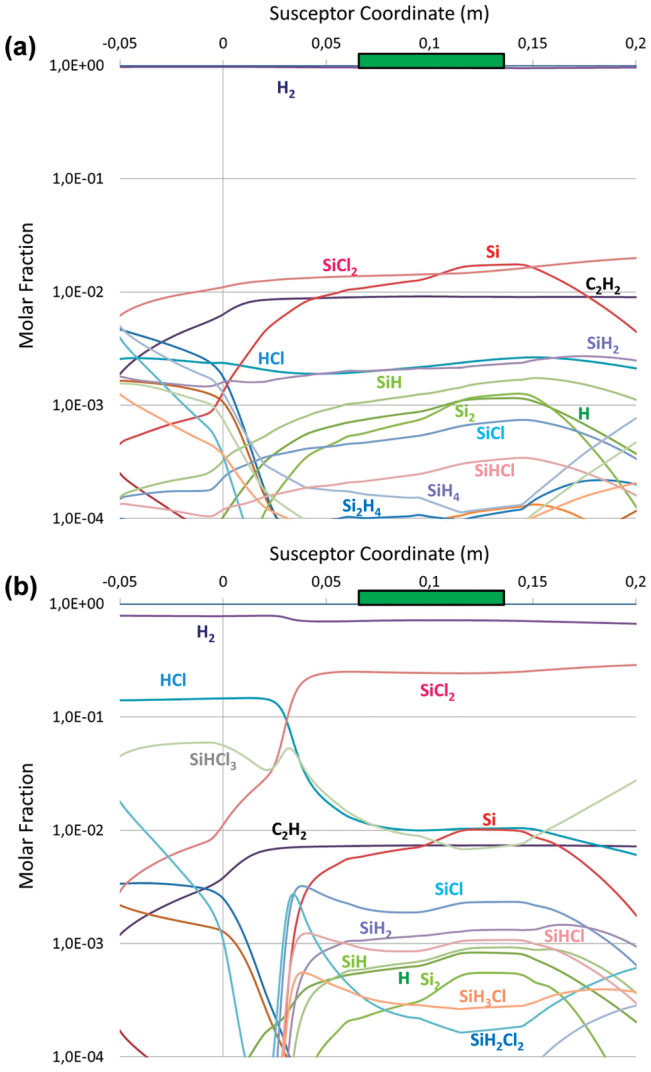

Figure 5. Plot of the gas-phase composition for the SiH_4 + C_2H_4 + HCl chemistry at 1600 °C with two different Cl/Si ratios: (a) 0.5; (b) 10.

how the Cl/Si ratio is a very important parameter for the epitaxial growth of SiC. Not only does the chlorine help to prevent the formation of silicon droplets which enables growth at higher growth rates, but also, it helps to get a more uniform gas phase composition, which is extremely important in order to produce layers uniform in thickness and doping profiles on large substrates. The experimental results considered in this study were always obtained only on small samples because the reaction chamber was small. An experimental confirmation of what is discussed above could come from epitaxial growth on large area substrates. Yet, it has been experimentally noticed how high Cl/Si ratios lead to uniform morphology when growing on on-axis 4H-SiC substrates.[44,45] This is a demonstration of a uniform gas phase composition along the reaction chamber.

Another important fact needs to be pointed out regarding the lower values of C/Si achieved by increasing the amount of chlorine in the systems. This confirms what we speculated in previous studies[38,39] that very high Cl/Si ratios make the gas phase even more silicon rich, which indeed helps the growth on on-axis substrates.

Precursor Concentration. A simple comparison between the case of Si/H_2 = 0.15% and 0.66% does not bring any relevant conclusion. As expected, the amounts of all the species increase

dx.doi.org/10.1021/cg201684e | Cryst. Growth Des. 2012, 12, 1977−1984

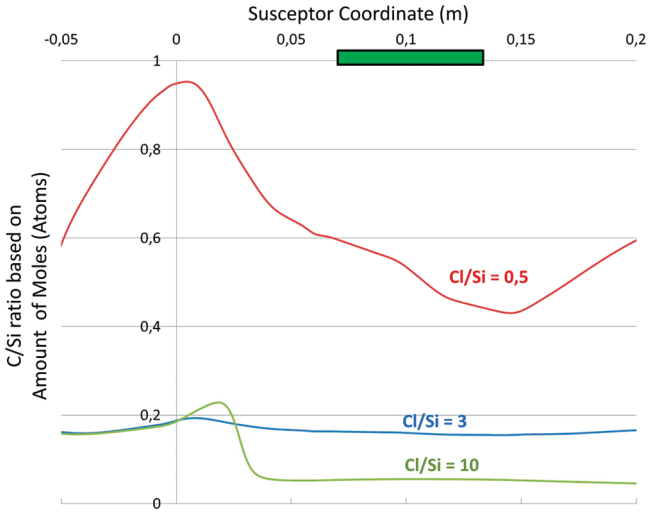

Figure 6. Plot of the gas-phase C/Si ratio along the susceptor coordinates for different Cl/Si ratios: 0.5 − 3 − 10. The precursors are SiH_4 + C_2H_4 + HCl.

in the gas-phase, maybe with the only advantage of increasing the gap between the concentration of $SiCl_2$ and Si, which should further inhibit the formation of silicon clusters. However, this has never been confirmed nor contradicted by experimental results. It is difficult to make any statements about this from the experimental results since the morphology of the layers grown at very high growth rates will deteriorate due to other phenomena, such as a not high enough adatom surface mobility for the increased supply of molecules from the gas-phase. The C/Si ratio trends obtained by simulations actually contradict the experimental results. While our calculations show a lower C/Si ratio at the higher precursor concentration, we have found from experimental results that lower C/Si ratios should be used to get good epilayer morphology. This is probably due to other reasons, again maybe due to surface mobility issues at enhanced growth rates, or due to the need for integrating surface reactions in the model.

4. CONCLUSION

Simulations of gas-phase reactions occurring in epitaxial growth of SiC have been performed and compared to experimental results. Although solid-phase reactions were not included in the model, the resulting model gave good explanations on the effect of several growth parameters, such as precursor choice, growth temperature, Cl/Si ratio, and precursor concentration.

The results of the simulations indicated that the gas-phase chemistry of carbon intermediates is very simple, while that of silicon intermediates is affected by several parameters. The efficiency of chlorinated molecules, such as CH_3SiCl_3 and $SiHCl_3$, is further confirmed as observed experimentally. Low temperatures lead to an increased complexity in the gas-phase chemistry, on account of the presence of more carbon intermediates, and of the risk of nucleation in the gas phase. The Cl/Si ratio shows a distinct effect on the gas-phase composition of silicon species, which not only prevents the formation of silicon droplets, but also favors a more uniform C/Si ratio along the susceptor coordinates.

AUTHOR INFORMATION

Corresponding Author

*E-mail: leonestefano@hotmail.com. Phone: + 4613288955. Fax: + 4613142337.

Notes

The authors declare no competing financial interest.

ACKNOWLEDGMENTS

The Swedish Energy Agency (Grant No. 32917-1) and the Swedish Research Council are gratefully acknowledged for financial support.

The authors are thankful to Dr. Henrik Pedersen, Dr. Urban Forsberg, and Milan Yazdanfar for interesting discussions and contributions on the topic.

REFERENCES

(1) Ito, M.; Storasta, L.; Tsuchida, H. *Appl. Phys. Express* **2008**, *1*, 015001.
(2) Pedersen, H.; Leone, S.; Henry, A.; Beyer, F. C.; Darakchieva, V.; Janzén, E. *J. Cryst. Growth* **2007**, *307*, 334−340.
(3) Crippa, D.; Valente, G. L.; Ruggiero, A.; Neri, L.; Reitano, R.; Calcagno, L.; Foti, G.; Mauceri, M.; Leone, S.; Pistone, G.; Abbondanza, G.; Abagnale, G.; Veneroni, A.; Omarini, F.; Zamolo, L.; Masi, M.; Roccaforte, F.; Giannazzo, F.; Di Franco, S.; La Via, F. *Mater. Sci. Forum* **2005**, *483−485*, 67−71.
(4) Meyers, R. L.; Shishkin, Y.; Kordina, O.; Saddow, S. E. *J. Cryst. Growth* **2005**, *285*, 486−490.
(5) Leone, S.; Henry, A., Janzén, E.; Nishizawa, S. *J. Cryst. Growth*. DOI:10.1016/j.jcrysgro.2011.09.061.
(6) Kojima, K.; Ito, S.; Senzaki, J.; Okumura, H. *Mater. Sci. Forum* **2010**, *645−648*, 99−102.
(7) Pedersen, H.; Leone, S.; Henry, A.; Lundskog, A.; Janzén, E. *Phys. Status Solidi (Rap. Res. Lett.)* **2008**, *2* (6), 278−280.
(8) La Via, F.; Galvagno, G.; Foti, G.; Mauceri, M.; Leone, S.; Vecchio, C.; Pistone, G.; Abbondanza, G.; Veneroni, A.; Masi, M.; Valente, G. L.; Crippa, D. *Chem. Vap. Deposition* **2006**, *12*, 509−515.
(9) Fanton, M.; Skowronski, M.; Snyder, D.; Chung, H. J.; Nigam, S.; Weiland, B.; Huh, S. W. *Mat. Sci. Forum* **2004**, *457−460*, 87−90.
(10) Chowdhury, I.; Chandrasekhar, M. V. S.; Klein, P. B.; Caldwell, J. D.; Sudarshan, T. *J. Cryst. Growth* **2011**, *316*, 60.
(11) Dhjanaraj, G.; Dudley, M.; Chen, Y.; Ragothamachar, B.; Wu, B.; Zhang, H. *J. Cryst. Growth* **2006**, *287*, 344−348.
(12) Pedersen, H.; Beyer, F. C.; Hassan, J.; Henry, A.; Janzén, E. *J. Cryst. Growth* **2009**, *311*, 1321.
(13) Pedersen, H.; Beyer, F. C.; Henry, A.; Janzén, E. *J. Cryst. Growth* **2009**, *311*, 3364.
(14) Meziere, J.; Ucar, M.; Blanquet, E.; Pons, M.; Ferret, P.; Di Cioccio, L. *J. Cryst. Growth* **2004**, *267*, 436.
(15) Danielsson, Ö.; Henry, A.; Janzén, E. *J. Cryst. Growth* **2002**, *243*, 170.
(16) Nishizawa, S.; Pons, M. *Chem. Vap. Deposition* **2006**, *12*, 516.
(17) Allendorf, M. D. *J. Electrochem. Soc.* **1993**, *140*, 747.
(18) Petrov, G. M.; Giuliani, J. L. *J. Appl. Phys.* **2001**, *90*, 619.
(19) Stinespring, C. D.; Wormhoudt, J. C. *J. Cryst. Growth* **1988**, *87*, 481.
(20) Veneroni, A.; Omarini, F.; Masi, M. *Cryst. Res. Technol.* **2005**, *40*, 972−975.
(21) Fiorucci, A.; Moscatelli, D.; Masi, M. *J. Cryst. Growth* **2007**, *303*, 345−348.
(22) Fiorucci, A.; Moscatelli, D.; Masi, M. *J. Cryst. Growth* **2007**, *303*, 349−351.
(23) Fischman, G. S.; Petuskey, W. T. *J. Am. Ceram. Soc.* **1985**, *68* (4), 185−190.
(24) Makarov, Y. N.; Talalaev, R. A.; Vorob'ev, A. N.; Ramm, M. S.; Bogdanov, M. V. *Mater. Sci. Forum* **2009**, *600−603*, 51.
(25) Veneroni, A.; Masi, M. *Chem. Vap. Deposition* **2006**, *12*, 562.
(26) Veneroni, A.; Masi, M. *Electrochem. Soc. Transact.* **2007**, *2*, 11.

(27) Fiorucci, A.; Moscatelli, D.; Masi, M. *Surf. Coat. Technol.* **2007**, *201*, 8825.
(28) Wang, R.; Ma, R. *J. Cryst. Growth* **2007**, *308*, 189.
(29) Wang, R.; Ma, R. *J. Cryst. Growth* **2008**, *310*, 4248.
(30) Wang, R.; Ma, R. *J. Thermophys. Heat Transfer* **2008**, *22*, 555.
(31) Wang, R.; Ma, R.; Dudley, M. *Ind. Eng. Chem. Res.* **2009**, *48*, 3860.
(32) Nishizawa, S. *J. Cryst. Growth* **2009**, *311*, 871−874.
(33) Chichignoud, G.; Ucar-Morais, M.; Pons, M.; Blanquet, E. *Surf. Coat. Technol.* **2007**, *201*, 8888−8892.
(34) Nigam, S.; Chung, H. J.; Polyakov, A. Y.; Fanton, M. A.; Weiland, B. E.; Snyder, D. W.; Skowronski, M. *J. Cryst. Growth* **2005**, *284*, 112.
(35) Nigam, S.; Chung, H. J.; Huh, S. W.; Grim, J.; Polyakov, A. Y.; Fanton, M. A.; Weiland, B. E.; Snyder, D. W.; Skowronski, M. *Mater. Sci. Forum* **2006**, *527*−*529*, 27.
(36) http://www.esi-cfd.com/
(37) Leone, S.; Beyer, F. C.; Pedersen, H.; Andersson, S.; Kordina, O.; Henry, A.; Janzén, E. *Thin Solid Films* **2011**, *519*, 3074−3080.
(38) Leone, S.; Pedersen, H.; Henry, A.; Kordina, O.; Janzén, E. *J. Cryst. Growth* **2009**, *312*, 24−32.
(39) Leone, S.; Beyer, F. C.; Henry, A.; Hemmingsson, C.; Kordina, O.; Janzén, E. *Cryst. Growth Des.* **2010**, *10*, 3743−3751.
(40) http://webbook.nist.gov/chemistry/
(41) Henry, A.; Leone, S.; Beyer, F. C.; Pedersen, H.; Kordina, O.; Andersson, S.; Janzén, E. *Physica B*, in press.
(42) Pedersen, H.; Leone, S.; Kordina, O.; Henry, A.; Nishizawa, S.; Koshka, Y.; Janzén, E. to be published on *Chem. Rev.*, DOI: 10.1021/cr200257z.
(43) Lewis, T. J. *Mater. Res. Bull.* **1969**, *4*, 321−330.
(44) Leone, S.; Pedersen, H.; Henry, A.; Kordina, O.; Janzén, E. *Mater. Sci. For.* **2009**, *600*−*603*, 107−110.
(45) Leone, S.; Beyer, F. C.; Pedersen, H.; Kordina, O.; Henry, A.; Janzén, E. *Cryst. Growth Des.* **2010**, *10* (12), 5334−5340.